Cellular Physiology and Biochemistry

Cell Physiol Biochem 2018;45:1986-1998
DOI: 10.1159/000487975
Published online: March 08, 2018
Accepted: December 12, 2017

Original Paper

Analysis of Long Noncoding RNA and mRNA Expression Profiles in IL-9-Activated Astrocytes and EAE Mice

Xiaomei Liu[a,b] Qing Zhang[c] Weixiao Wang[b] Dongjiao Zuo[b] Jing Wang[b] Feng Zhou[b] Liping Niu[b] Xiangyang Li[b] Suping Qin[b] Yanbo Kou[b] Fanyun Kong[b] Wei Pan[b] Yugang Wang[b] Dianshuai Gao[d] Hong Sun[e] Jessica M. Meves[f] Kuiyang Zheng[b] Renxian Tang[b]

[a]Jiangsu Key Laboratory of New Drug Research and Clinical Pharmacy, Xuzhou Medical University, Xuzhou, Jiangsu, [b]Jiangsu Key Laboratory of Immunity and Metabolism, Department of Pathogen Biology and Immunology and Laboratory of Infection and Immunity, Xuzhou Medical University, Xuzhou, Jiangsu, [c]Clinical Laboratory of Xuzhou Tumor Hospital, Xuzhou, Jiangsu, [d]Department of Neurobiology and Anatomy, Xuzhou Medical University, Xuzhou, Jiangsu, [e]Department of Physiology, Xuzhou Medical University, Xuzhou, Jiangsu, China; [f]Department of Neurosciences, University of California San Diego, School of Medicine, La Jolla, CA, USA

Key Words
Multiple sclerosis • Experimental autoimmune encephalomyelitis • LncRNAs • Astrocytes • IL-9

Abstract
Background/Aims: Multiple sclerosis (MS) is an autoimmune disease in the central nervous system associated with demyelination and axonal injury. Astrocyte activation is involved in the pathogenesis of MS and experimental autoimmune encephalomyelitis (EAE), an animal model of MS. This study was designed to find potential lncRNAs in EAE mice and activated astrocytes. ***Methods:*** we performed microarray analysis of lncRNAs from the brain tissues of EAE mice and primary mouse astrocytes treated with IL-9(50 ng/ml). 12 lncRNAs were validated through real-time PCR. Gene ontology and KEGG pathway analysis were applied to explore the potential functions of lncRNAs. ***Results:*** Differentially expressed 3300 lncRNAs and 3250 mRNAs were in the brain tissues of EAE mice, and 3748 lncRNAs and 3332 mRNAs were in activated astrocytes. Notably, there were 2 co-up-regulated lncRNAs and 3 co-down-regulated lncRNAs both in the brain tissues of EAE mice and in activated astrocytes, including Gm14005, Gm12478, mouselincRNA1117, AK080435, and mouselincRNA0681, which regulate the ER calcium flux kinetics, zinc finger protein and cell apoptosis. Similarly, there were 7 mRNAs co-up-regulated and 2 mRNAs co-down-regulated both *in vivo* and *in vitro*. Gene ontology and KEGG pathway analysis showed that the biological functions of differentially expressed mRNAs were associated with metabolism, development and inflammation. The results of real-time PCR validation were consistent with the data from the microarrays. ***Conclusions:*** Our

X. Liu and Q. Zhang contributed equally tot this work.

Kuiyang Zheng
and Renxian Tang

Jiangsu Key Laboratory of Immunometabolism and Department of Pathogen Biology and Immunology, Xuzhou Medical University, 209 Tongshan Road, Xuzhou, Jiangsu (China); Tel. +86-516-83262124, E-Mail zky02@163.com, tangrenxian-t@163.com

data uncovered the expression profiles of lncRNAs and mRNAs *in vivo* and *in vitro*, which may help delineate the mechanisms of astrocyte activation during MS/EAE process.

Introduction

Multiple sclerosis (MS) is a devastating disease of the central nervous system (CNS), and is characterized by activated autoreactive $CD4^+$T cells that infiltrate into the CNS and mediate inflammation, demyelination, progressive axonal degradation and reactive astrogliosis [1, 2]. MS and its animal model, experimental autoimmune encephalomyelitis (EAE), had initially been thought to be Th1-mediated diseases. Recent studies provide strong evidence that Th17 and Th9 cells also play important roles in the pathogenesis of MS/EAE [3]. IL-9, a signature cytokine produced by Th9 and Th17 cells, is able to amplify Th17 development via a positive feedback loop [3]. Furthermore, IL-9 promotes Th17 cell migration into the CNS through the activation of astrocytes, and blocking IL-9 with neutralizing antibodies ameliorates the EAE [4, 5].

Astrocytes, the major glial cell type within the CNS, regulate neuronal function and participate in the formation of the blood-brain barrier (BBB) [6]. Furthermore, astrocytes have the capacity to interact with the peripheral immune system by recruiting leukocytes into the CNS [7]. Reactive astrocytosis is a prominent feature in inflammatory condition that occurs during MS and EAE. Experimental evidence suggests that astrocyte activation contributes to a more severe course of MS and EAE characterized by an increased expression of proinflammatory cytokines and chemokines as well as pronounced demyelination [8-10]. In response to IL-9 treatment, astrocytes increase chemokine production to facilitate T cell recruitment to the CNS [5]. However, the mechanisms by which astrocyte activation contribute to MS/EAE after IL-9 stimulation are not fully understood.

Long non-coding RNAs (lncRNAs) have been defined as transcripts of >200 nucleotides without protein coding capacity. Although genomic studies indicated that approximately two-thirds of genomic DNA are pervasively transcribed, less than 2% of mRNAs are ultimately translated into proteins [11, 12]. Based on the position of lncRNA in the genome relative to protein-coding genes, lncRNAs are divided into five categories: sense, antisense, intronic, intergenic and bidirectional [13]. LncRNAs are widely involved in various biological and physiological processes including chromatin remodeling, gene transcription, RNA splicing and protein transport, and directly linked to human diseases including various cancers, and neurological disorders [14-16]. It has been reported that lncRNAs regulate the gene expression in the immune system and in autoimmune disease [17, 18]. However, the roles of lncRNAs in the process of MS/EAE are still unclear.

In the present study, we analyzed the lncRNA and mRNA expression landscape of the brain tissues from EAE mice and activated astrocytes stimulated by IL-9 *in vitro*. Our results suggest the potential roles of lncRNAs in regulating astrocyte functions during the process of EAE.

Materials and Methods

Animal ethics statement

All experimental procedures described in the present study were conducted according to the Provision and General Recommendation of the Chinese Laboratory Association. The protocol was approved by the Institutional Animal Care and Use Committee of Xuzhou Medical University. The study was approved by the Ethical Committee for Xuzhou Medical University.

Animal model of EAE

C57BL/6 mice were obtained from Nanjing University Laboratory Animal Center. Mice were housed in clean plastic cages with the temperature of 25 ± 1 ºC and humidity of 55-65 % and maintained under specific

pathogen-free conditions. EAE models were induced according to our previously published procedure [19]. Briefly, 6- to 8-wk-old C57BL/6 female mice randomly divided into two groups (n=10 each group): One was injected by s.c. immunization with 200 μg MOG_{35-55} peptide emulsified in complete Freund's adjuvant (CFA, Sigma) containing 5 mg/ml heat-killed mycobacterium tuberculosis (H37Ra strain, Difco). In addition, 200 ng of pertussis toxin (Invitrogen) in PBS was i.p. injected on day 0 and day 2 after MOG_{35-55} treatment. Mice were monitored daily for clinical signs of EAE and graded on a scale of increasing severity from 0 to 5: 0, no clinical signs; 1, limp tail; 2, paraparesis (weakness, incomplete paralysis of 1 or 2 hind limbs); 3, paraplegia (complete paralysis of 2 hind limbs); 4, paraplegia with fore limb weakness or paralysis; and 5, moribund state or death. Another group was injected with the same volume of PBS, as negative control (NC). Mice were sacrificed after anesthetization by i.p. injection of a mixture of ketamine (120 mg/kg) and xylazine (60 mg/kg).

Primary mouse astrocyte cultures

Primary astrocytes from 0- to 1-day-old C57BL/6 mice were established as previously described [19]. Briefly, the cerebral cortices freed of meninges were dissected, minced and digested. After being washed twice in Dulbecco's Modified Eagle Medium F12 (DMEM/F12) containing 10% fetal bovine serum (FBS) and antibiotics, the cells were filtrated through a 75 μm cell strainer and transferred to culture flasks pre-coated with 1mg/ml poly-L-lysine (Sigma) and cultured at 37°C with 5% CO_2. At complete confluence, flasks were shaken on an orbital shaker for 1 h (150 rpm at 37°C). The cultures were passed for 3 or 4 passages, and glial fibrillary acidic protein (GFAP, astrocytic marker) expression was evaluated via immunofluorescence assay.

Histopathology

Mice were perfusion-fixed with 4% paraformaldehyde in 0.1 M sodium phosphate buffer (pH 7.4) under anesthesia. Brains and spinal cords were removed quickly and further fixed with the same fixation solution overnight at 4 °C. The histological evaluation of brains and spinal cord tissues was performed on 4 μm paraffin-embedded sections stained with hematoxylin and eosin (H&E) or luxol fast blue (LFB) to assess inflammation or demyelination under microscopy. Ultrathin sections of spinal cord tissues were stained with uranyl acetate and lead citrate, and the ultrastructural changes were observed under electron microscopy (EM).

RNA extraction

Total RNA was isolated from the brain tissues of mice and the primary astrocytes according to manufactures instructions. RNA quantity and quality was measured using NanoDrop ND-1000 spectrophotometer (Thermo Fisher Scientific). The RNA integrity of each sample was assessed using standard denaturing agarose gel electrophoresis.

Determination of lncRNA and mRNA profiles in EAE mice and primary astrocytes

The expression profiles of lncRNAs and mRNAs in brain tissues of EAE mice and activated astrocytes were detected using Mouse LncRNA Microarray v2.0 (8 x 60K, Arraystar) by Kangchen Bio-tech (Shanghai, China), which includes 31, 423 lncRNA probes and 25, 376 coding transcripts probes. Microarray assays were also performed using pooled plasma, blood, liver, heart or cell samples [20, 21]. So RNAs from the pooled brain tissues from the control or EAE mice (4 mice in each group) and RNAs from astrocytes (DMEM/F12 control and IL-9 treatment) underwent microarray analysis. The acquired raw array images were processed by Agilent Feature Extraction software (version 11.0.1.1) and then normalized and analyzed by the GeneSpring GX v12.0 software package (Agilent Technologies). Differentially expressed lncRNAs and mRNAs were then identified through fold-change as well as P values calculated with *t*-test. The threshold for up- and down-regulation was fold change > 2.0 and p value < 0.05. Afterwards, Hierarchical Clustering was performed to display the distinguishable lncRNAs and mRNAs expression patterns among the samples.

Real-time PCR assay

The total RNA from the brain tissues of mice and cultured astrocytes was extracted with TRIzol reagent (Invitrogen). First-strand cDNAs were generated using PrimeScriptTM RT reagent kit (TaKaRa, Japan), and SYBR Premix Ex TaqTM based on real-time PCR (TaKaRa) were used to analyze the relative expression levels of the selected lncRNAs. The relative gene expression was calculated using the $2^{-\Delta\Delta}$CT method. The primers are listed in Table 1.

Functional group analysis

Gene ontology (GO) and KEGG analysis were applied to determine the roles of differentially expressed mRNAs in biological pathways using the standard enrichment computation method. The p value (Hypergeometric-P value) denotes the significance of the pathway correlated to the conditions. The recommend p-value cut-off is 0.05.

Statistical analysis

Data were presented as mean ± SD. Statistical significance of differences between groups was analyzed by nonparametric tests (K independent samples test) or one-way analysis of variance (ANOVA) when more than two groups were compared. GraphPad Prism 5.0 for Microsoft Windows was used to plot all graphs. The criterion for statistical significance was $P < 0.05$.

Results

Inflammatory cell infiltration and severe demyelination in EAE mice

The EAE model has been widely used in the investigation of the mechanisms underlying MS. Here, we also found that MOG_{35-55} peptide induced EAE mice showed increasing severity of clinical signs from scale 1 to 4 as time goes on (Fig. 1A). We then analyzed brain and spinal cord tissues from EAE mice on day 20 after MOG_{35-55} immunization (exhibiting clinical scale 4) by staining with hematoxylin and eosin (HE) and luxol fast blue (LFB), respectively. The results of HE staining showed that the EAE mice brain sections and spinal cord sections developed

Table 1. Primers for verification of lncRNAs by qRT-PCR

Primer Name	Sequence (5′ to 3′)	Length (bp)
ENSMUST00000119467	Fw TGCTAACGCAGCCTCTACTCG	198
	Rev TCCAGCCAGATTGTCTGTTTCAG	
AK033297	Fw GGCACAGAAGCATTTAGAGCG	231
	Rev GGTTAGCAGTTACTTCCTTTCCTCA	
ENSMUST00000119913	Fw ATCATCAAACCCGAAAGGAGC	145
	Rev AGTCACTGAAGCAGGGCAAGA	
ENSMUST00000075251	Fw TGAAGATTAAGTTTCGTGAAGAACC	244
	Rev TTGTTTCTATGACCATTGGAATCC	
ENSMUST00000062533	Fw TTTGACGGTTGTGATAGGAAGTTTG	129
	Rev AGAGCTTGGGTGGGTGTATGATT	
ENSMUST00000137239	Fw TCTGCTCATAGGAACTCTTGCTATC	130
	Rev CCTTGGAGAAATGGCTGACTT	
ENSMUST00000156666	Fw CCGTGGAAGAACTACTGAACAAGC	182
	Rev GCCTCATTCATCCCAAACTCG	
ENSMUST00000145143	Fw AGGGACCAAGACCAGAAGGAA	147
	Rev GGAATGTGAGGTATCTAAGGGAAGTA	
ENSMUST00000134472	Fw CACTGGCAGCAGGTCCATCTA	248
	Rev TCTTGCTAGTCTTGTCATTCCTGG	
uc008aid.1	Fw CCTGGCACTTTAACTTAGATGAGATT	258
	Rev GGTAGTAGTTGATGGATGGCTTGA	
uc008rso.1	Fw ACATCCAACAGCCCTCAGACA	298
	Rev TCGTCAAGAGCGACAGCAAAC	
ENSMUST00000149952	Fw GCCTCTGCCCAGTTACTTGGAG	157
	Rev CAGTTTGCCATCTGGTTACCCTAC	

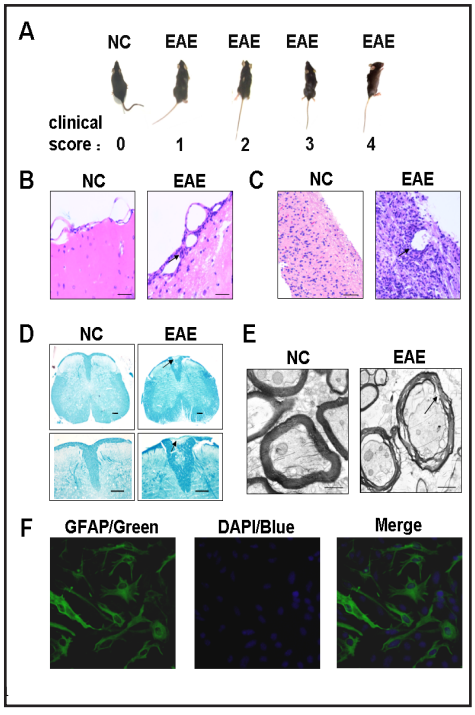

Fig. 1. Identification of EAE mouse model and cultured primary mouse astrocytes. (A) The clinical symptom of EAE mice was scored daily as described in materials and methods. (n = 10 mice per group). (B) Paraffin sections of the brain tissues in EAE on day 20 after MOG_{35-55} immunization (average clinical scale 4) were stained with H&E to determine inflammatory cell infiltrations (black arrows, n = 4 mice). (C) Sections of the spinal cords in EAE mice stained with H&E. Scale bars, 50 μm. (D) Spinal cord sections of EAE mice exhibiting as demyelination with luxol fast blue (LFB) staining (black arrows), whereas no demyelination was seen in the negative control (NC) group. Scale bars, 50 μm. (E) Spinal cords of the mice with EAE (average clinical scale 4) under electron microscopy (EM) exhibited loose and disrupted myelination (arrow). Scale bars, 1μm. (F) Immunofluorescence for GFAP in cultured primary mouse astrocytes. The cell nuclei were stained by DAPI.

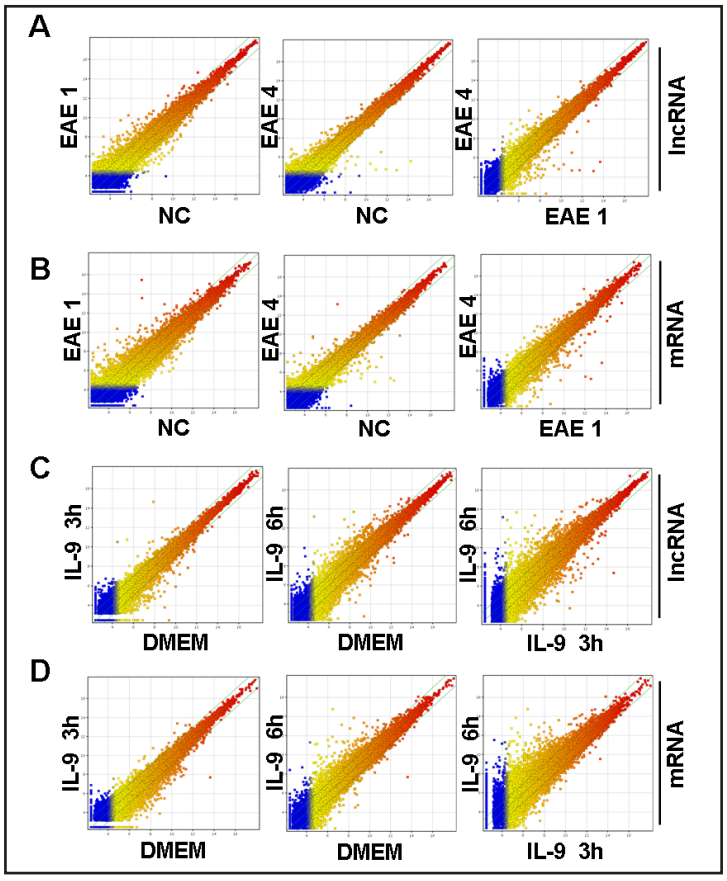

Fig. 2. Scatter plot comparing global lncRNA or mRNA gene expression profiles in vivo and in vitro. lncRNA expression profiles (A) and mRNA expression profiles (B) changed in the brain tissues of EAE mice (clinical scale 1 and scale 4) and NC mice. lncRNA (C) and mRNA (D) expression profiles in the activated astrocytes induced by IL-9 (at 3 h and 6 h) and DMEM/F12 control group. The values of X-axis and Y-axis in the scatter-plot were the normalized signal values of each sample (log 2 scaled). The green lines are fold change lines (the default fold change value given is 2.0). The lncRNAs and mRNA above the top green line and below the bottom green line indicate > 2.0-fold change, compared to the control.

prominent inflammatory cell infiltration, which did not occur in PBS-treated mice (Fig. 1B and C). Furthermore, LFB staining demonstrated that the spinal cords of EAE mice had severe demyelination (Fig. 1D). Specifically, the myelin sheaths of the EAE mice were ruptured and disintegrated under EM (Fig. 1E). For astrocyte isolation, at least $GFAP^+$ cells occupied 95% in cultured mouse primary astrocytes under Fluorescence microscope (Fig. 1F).

Differential LncRNA and mRNA expression in the brain tissues from EAE mice and primary mouse astrocytes treated with IL-9

To detect differentially expressed lncRNAs in the brain tissues of EAE mice and activated mouse primary astrocytes, we performed a genome-wide analysis of lncRNA and mRNA expression in the brain tissues of EAE mice (clinical scale 1 and scale 4) and matched NC mice. Meantime, we also analyzed the lncRNA and mRNA expression profiles of non-activated astrocytes (DMEM/F12 control group) and activated astrocytes induced by IL-9 (50 ng/ml, at 3 h and 6 h). We first obtained a graphical overview of the expression signatures of lncRNAs and mRNAs by using scatter plot analyses, which showed that a large number of lncRNAs and mRNAs were differentially expressed in EAE and NC mice (Fig. 2A and B). Similarly, many differentially expressed lncRNAs and mRNAs were observed between the activated astrocytes and DMEM control (Fig. 2C and D).

We then further analyzed differential expression of lncRNAs and mRNAs with fold change > 2 (the criteria q-value < 0.05) in EAE mice or activated astrocytes compared with NC mice or DMEM control, respectively. Results displayed that 1, 850 lncRNAs and 1, 642 mRNAs were up-regulated, and 1, 450 lncRNAs and 1, 608 mRNAs were down-regulated in the brain tissues of EAE mice (Fig. 3A). Meanwhile, 1, 584 lncRNAs and 1, 435 mRNAs were up-regulated, and 2, 164 lncRNAs and 1, 897 mRNAs were down-regulated in the astrocytes stimulated by IL-9 stimulation for 3 h and 6 h (Fig. 3 B). Notably, there were 2 lncRNAs co-up-regulated and 3 lncRNAs co-down-regulated both in the brain tissues from EAE mice and in the activated

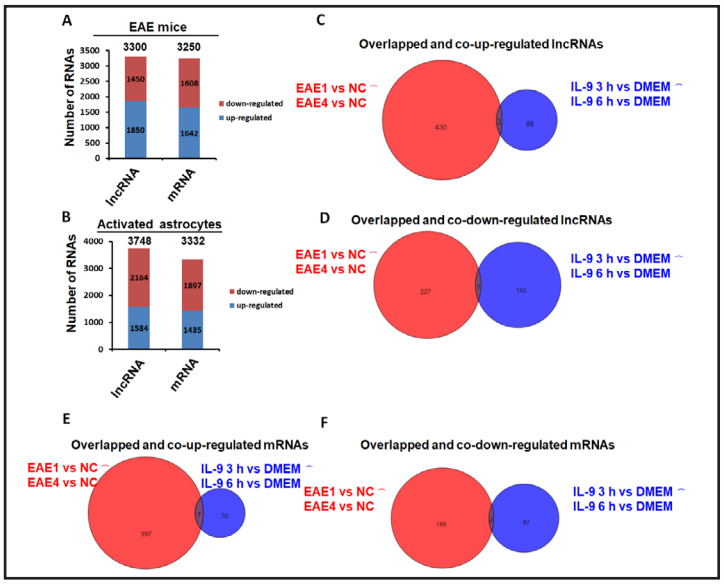

Fig. 3. Differentially expressed lncRNAs and mRNAs in EAE mice or the activated astrocytes. (A) and (B) Analysis of numbers of significantly expressed lncRNAs and mRNAs. (C) and (D) Overlapping and differentially expressed lncRNAs both in vivo and in vitro. (E) and (F) Overlapping and differentially expressed mRNAs both in vivo and in vitro.

astrocytes (Table 2; Fig. 3C and D). Interestingly, the 5 differentially co-expressed lncRNAs *in vivo* and *in vitro* are belong to intergenic lncRNAs, and regulate the ER calcium flux kinetics, zinc finger protein, cell apoptosis and multifunctional serine/threonine protein phosphatases. Similarly, there were 7 mRNAs co-up-regulated and 2 mRNAs co-down-regulated both in the brain tissues from EAE mice and in activated astrocytes (Table3; Fig. 3E and F). The list of the top 20 differentially expressed lncRNAs *in vivo* and *in vitro* identified by microarray analysis is shown in Table 4-7. Furthermore, the top 20 up-regulated and down-regulated mRNA transcripts *in vivo* and *in vitro* are displayed in Table 8-11, respectively.

Table 2. Overlapped and differentially expressed lncRNAs

Gene symbol	RNA lenth	Folds EAE 1	Folds EAE 4	Folds IL-9 (3 h)	Folds IL-9 (6h)
Gm14005	356	3.9003537	2.4139466	3.1771016	2.8205125
Gm12478	353	2.2662761	2.7239292	2.1583462	2.032246
mouselincRNA1117	6275	-2.510708	-2.0096638	-3.1769779	-2.340342
AK080435	469	-2.8653665	-2.0491805	-2.4332886	-5.2294827
mouselincRNA0681	110	-2.0130742	-2.327964	-4.0724044	-5.2345243

Table 3. Overlapped and differentially expressed mRNAs

Gene symbol	Folds EAE 1	Folds EAE 4	Folds IL-9 (3 h)	Folds IL-9 (6h)
Cxcl1	12.778519	2.6610117	2.6701224	3.0138001
Gpr84	2.6615167	2.2510245	4.5140734	2.345894
Nfkb	2.6183925	2.419111	3.7595193	2.747609
Cxcl10	20.973085	33.02361	3.1710043	7.465219
S100a	48.44693	29.814625	2.2521923	2.147164
Ccl2	3.637598	6.4596	3.1756024	9.821831
Tnf	3.582732	2.8130655	5.9117227	4.6778245
Ttc5	-6.4337587	-3.4288063	-7.556124	-7.4247823
Calm3	-13.898376	-4.7527223	-6.8642373	-2.8599412

Importantly, some inflammatory cytokines, including CXCL10 (IP-10), CCL2, CXCL2 and TNF were detected in the up-regulated mRNAs *in vivo* (clinical scale 1 and scale 4, Table 8) or *in vitro* (at 3 h and 6 h induced by IL-9, Table 10). These data suggest that MS/EAE is associated with the changes of lncRNAs and mRNAs in the brain tissues and the activated astrocytes.

Validation of the microarray data using real-time PCR

To further validate the accuracy of microarray data, we randomly selected 12 lncRNAs from the differentially expressed lncRNAs, including 6 that were co-up-regulated (ENSMUST00000119467, AK033297, ENSMUST00000119913, ENSMUST00000075251, ENSMUST00000062533 and ENSMUST00000137239) and 6 co-down-regulated (ENSMUST00000156666, ENSMUST00000145143, ENSMUST00000134472, uc008rso.1, uc008aid.1 and ENSMUST00000149952), and detected their expression through real-time PCR assay. As shown in Fig. 4A, ENSMUST00000119467, AK033297 and ENSMUST00000119913 expression were significantly increased, and ENSMUST00000156666,

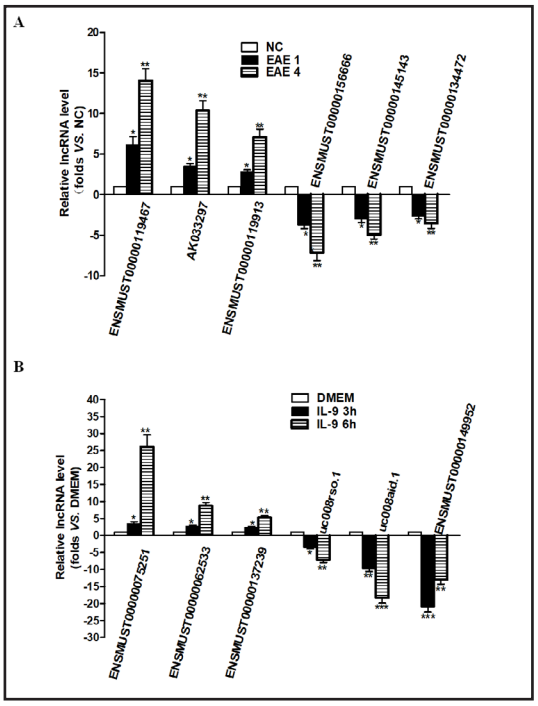

Fig. 4. Real-time PCR validation of differentially co-expressed lncRNAs in EAE mice or the activated astrocytes. 12 lncRNAs were randomly chosen for real-time PCR validation in vivo and in vitro. (A) The expressions of lncRNA ENSMUST00000119467, AK033297 and ENSMUST00000119913 were significantly increased in the brain tissues of EAE mice with clinical scale 1 and in scale 4, meanwhile, ENSMUST00000156666, ENSMUST00000145143 and ENSMUST00000134472 expression were obviously decreased in EAE mice. **P<0.01, ***P<0.001 vs NC (n = 3 mice per group). (B) The expressions of lncRNA ENSMUST00000075251, ENSMUST00000062533 and ENSMUST00000137239 were significantly up-regulated in activated astrocytes stimulated by IL-9 for 3 h and 6 h, while uc008rso.1, uc008aid.1, ENSMUST00000149952 were markedly down-regulated in activated astrocytes. *P<0.05, **P<0.01, ***P<0.001 vs DMEM. Error bars represent means ± SD.

ENSMUST00000145143 and ENSMUST00000134472 expression were significantly decreased in the brain tissues of EAE mice with clinical scale 1 and scale 4, compared with NC control. The expression levels of the ENSMUST00000075251, ENSMUST00000062533 and ENSMUST00000137239 were markedly up-regulated, and uc008rso.1, uc008aid.1, ENSMUST00000149952 were significantly down-regulated in activated astrocytes stimulating with IL-9 for 3 h and 6 h, compared with DMEM control (Fig. 4B). Overall, these results confirmed the accuracy of microarray data obtained from analysis of pooled samples.

Class distribution of changed lncRNAs

According to the relative location of lncRNA to coding genes, we analyzed class distribution of differentially co-expressed LncRNAs. Among the co-expressed lncRNAs in the brain tissues of EAE mice with clinical scale 1 and scale 4, intergenic lncRNAs were the largest category along with 270 up-regulated and 150 down-regulated lncRNAs. Secondly, among antisense lncRNAs 80 were up-regulated and 57 were down-regulated. Thirdly, among sense lncRNAs 67 were upregulated and 20 were down-regulated. Bidirectional lncRNAs were the smallest

Table 4. Top 20 overlapped and up-regulated lncRNAs of the brain tissues from EAE mice with clinical scale 1 and 4

lncRNA seqname	RNA length	up-regulated fold	
		Scale1/NC	Scale 4/NC
ENSMUST00000119669	663	7.85589	10.23717
uc008use.1	3335	8.610238	9.648406
ENSMUST00000119467	1274	4.3121204	9.547864
AK033297	3620	2.6846502	8.161776
NR_033450	2051	8.633687	8.022282
uc009spu.1	1729	22.872778	7.0451984
AK045052	1766	6.6805325	7.0031447
uc008rso.1	778	6.1572304	6.500624
MM9LINCRNAEXON11637+	1180	5.5882964	6.351306
uc007rdz.1	1529	6.1322365	6.0852413
AK008216	1208	10.930726	6.014869
ENSMUST00000135792	424	6.7050333	5.8834567
AK141778	1953	3.3443995	5.8223014
ENSMUST00000037976	913	5.596207	5.7913294
AK136771	2813	4.8559976	5.628442
humanlincRNA2345-	11309	10.116245	5.574991
ENSMUST00000160565	1414	5.6017933	5.5404854
ENSMUST00000153719	726	5.106356	5.521596
uc.150+	262	5.8136806	5.2537236
AK133322	3838	4.8335	5.206456

Table 5. Top 20 overlapped and down-regulated lncRNAs of the brain tissues from EAE mice with clinical scale 1 and 4

lncRNA seqname	RNA length	down-regulated fold	
		Scale1/NC	Scale 4/NC
ENSMUST00000163836	420	-40.030895	-37.572098
uc009iwa.	832	-7.5178285	-7.8960743
AK020153	710	-6.851927	-5.964112
CN673952	517	-5.260042	-5.617605
ENSMUST00000156666	1319	-3.937882	-5.388637
AK082604	2334	-2.9760792	-4.963089
AK006093	270	-5.834375	-4.864372
AF346502	325	-4.7329516	-4.8320174
AK019721	538	-4.6150265	-4.790841
AK042092	2251	-4.2353625	-4.676630
AK015350	1005	-4.1139274	-4.5655036
BC051648	1091	-5.0416775	-4.529922
ENSMUST00000145143	560	-2.9116006	-4.4599357
uc.394+	202	-3.5275517	-4.4599357
AK034340	3369	-12.039054	-4.446819
ENSMUST00000120738	412	-4.793811	-4.224718
AK131760	1316	-3.0181768	-4.16362
AK033086	2497	-3.5453696	-3.9964097
ENSMUST00000148691	710	-4.1512413	-3.933257
AK155134	3476	-3.5343256	-3.8350103

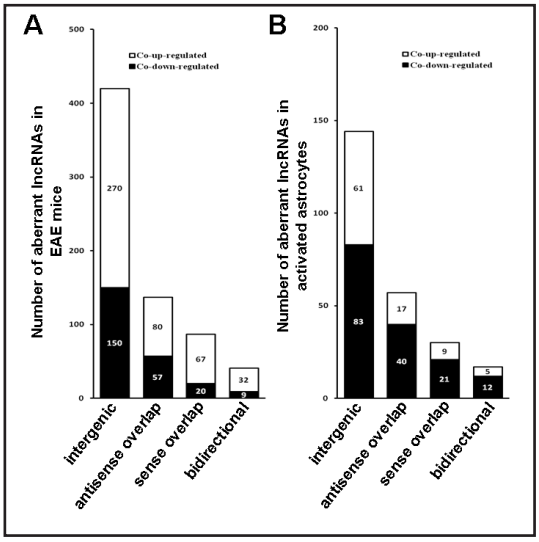

Fig. 5. Distribution of various types of lncRNAs. Co-expressed numbers of intergenic lncRNAs, antisense overlap lncRNAs, sense overlap lncRNAs and bidirectional lncRNAs were analyzed in the brain tissues of EAE mice with clinical scale 1 and scale 4 (A) and in activated astrocytes stimulated by IL-9 for 3 h and 6 h (B).

category including 32 up-regulated and 9 down-regulated lncRNAs (Fig. 5A). Similarly, as shown in Fig. 5B, among the co-expressed lncRNAs in the activated mouse primary astrocytes stimulated with IL-9 for 3 h and 6 h, intergenic lncRNAs were still the largest category, including 61up-regulated and 83 down-regulated lncRNAs. The other differentially co-expressed lncRNAs included 57 antisense lncRNAs (17 up-regulated and 40 down-regulated), 30 sense lncRNAs (9 up-regulated and 21 down-regulated), and 17 bidirectional lncRNAs (5 up-regulated and 12 down-regulated).

Go and KEGG pathway analysis

To further explore potential molecular mechanism in MS, we ran GO and KEGG Pathway analysis of differentially expressed genes in the brain tissues of EAE mice and activated astrocytes. GO analysis indicated that differentially co-up-regulated transcripts were biological regulation, metabolism regulation and biological process regulation in the brain tissues of EAE mice and activated astrocytes (Fig. 6A and B). Furthermore, differentially co-down-regulated genes were mainly associated with cell development in the brain tissues of EAE mice and activated astrocytes (Fig. 6C and D).

Table 6. Top 20 overlapped and up-regulated lncRNAs in mouse astrocytes stimulated with IL-9 (50 ng/ml) for 3 h and 6 h *in vitro*

lncRNA seqname	RNA length	up-regulated fold	
		3 h/DMEM	6 h/DMEM
ENSMUST00000075251	522	3.9349897	40.166023
ENSMUST00000062533	606	2.0524364	12.538993
AK083446	2226	2.2753801	12.145436
humanlincRNA0889+	23120	3.0090966	8.693425
MM9LINCRNAEXON11983+	1278	2.2759817	7.63561962
ENSMUST00000165402	699	3.0055168	4.8639135
ENSMUST00000137239	1475	2.0873954	4.690183
AK083633	1745	2.104949	4.188388
uc.480+	202	2.6271284	4.010122
uc008ydi.1	605	3.2122352	3.9657302
uc008ajj.1	364	3.383075	3.900578
MM9LINCRNAEXON12120+	360	2.537424	3.8664494
AK020497	977	2.0829475	3.858925
AK014172	761	2.4132385	3.7605712
AK146536	2999	2.801698	3.7465243
MM9LINCRNAEXON11883-	1673	7.5292897	3.7110455
ENSMUST00000129149	549	4.7973676	3.6296542
uc.30+	243	2.941384	3.5964377
AK014724	1450	2.270314	3.5466068
uc008ich.1	1068	2.039356	3.5054522

Table 7. Top 20 overlapped and down-regulated lncRNAs in mouse astrocytes stimulated with IL-9 (50 ng/ml) for 3 h and 6 h *in vitro*

lncRNA seqname	RNA length	down-regulated fold	
		3 h/DMEM	6 h/DMEM
MM9LINCRNAEXON10644-	529	-117.604935	-99.0716
AK136795	2457	-20.417713	-20.625822
uc008aid.1	2654	-12.142941	-20.602228
AK047651	1505	-16.56007	-16.410059
ENSMUST00000149952	435	-34.908175	-15.565921
AK039597	918	-12.962295	-14.543182
AK044317	1433	-11.480068	-12.880182
MM9LINCRNAEXON10750+	270	-12.000128	-12.189643
ENSMUST00000167046	1189	-11.106656	-11.7804575
AK140223	2651	-2.0036714	-11.718122
uc007ztt.1	4087	-7.7851024	-8.734577
uc008rso.1	778	-3.6056058	-8.127705
uc008lll.1	1020	-6.8208704	-7.652747
uc008jnj.1	2334	-5.3359036	-7.1349945
AK156979	3729	-2.875295	-7.0227046
MM9LINCRNAEXON10159+	424	-2.4457703	-6.8156323
AK146287	865	-4.4910707	-6.699524
ENSMUST00000098624	1317	-6.066518	-6.6513
MM9LINCRNAEXON10379+	406	-3.5663848	-6.1227465
AK020959	532	-2.0639613	-6.068381

Table 8. Top 20 overlapped and up-regulated mRNAs in the brain tissues of EAE mice with clinical scale 1 and 4

Gene symbol	Gene length	up-regulated fold	
		Scale 1/NC	Scale 4/NC
Ttr	1237	335.11658	68.372696
Cxcl10	1063	20.973085	33.02361
S100a8	392	48.44693	29.814625
Cfb	2767	36.640877	22.740374
Tmem102	1941	4.4589195	17.689392
Ch25h	1365	12.644377	10.278557
Olfr91	939	8.076411	9.904047
1110059M19Rik	1123	23.963148	9.76958
Ifi204	2302	8.120821	8.638965
Ccl5	579	6.5959787	8.330466
Gm14548	2130	14.441691	8.216907
Ccl12	537	6.719245	8.077436
Lcn2	853	12.209477	7.716298
H2-Q8	1183	6.778891	7.393144
Frmd6	4695	3.224566	7.015356
Ifi205	1613	9.347171	6.800729
Ccl2	806	3.637598	6.4596
Apobec3	2459	3.7751663	6.212857
Zbp1	781	8.288381	6.201317
Cd74	1239	10.382884	6.1446013

Table 9. Top 20 overlapped and down-regulated mRNAs in the brain tissues of EAE mice with clinical scale 1 and 4

Gene symbol	Gene length	down-regulated fold	
		Scale 1/NC	Scale 4/NC
Cux2	5133	-2.0224001	-50.37911
Cd300lb	2880	-15.030037	-15.786247
Hoxa9	2272	-8.497262	-11.213646
Dact3	2828	-14.50526	-7.4577813
Cep97	7904	-6.039256	-6.9138865
Ccdc136	3507	-4.752726	-6.1138263
Calm3	2233	-13.898376	-4.7527223
Ehmt1	5070	-2.5776749	-4.6222963
Gstt3	1873	-4.3256702	-4.578973
Dock1	6815	-4.7299695	-4.3923683
Stambpl1	1978	-14.772	-4.329778
Tgfbr2	4728	-5.0039163	-4.315667
Il17rc	2272	-3.4610384	-4.3087068
Men1	2644	-5.994871	-4.152673
Neurl4	5203	-5.317888	-4.1331754
Lepr	3407	-3.9306805	-4.1284456
Gm11710	852	-2.6119237	-4.0417027
Stk25	3254	-6.3022923	-4.024722
Rsad2	3785	-3.831459	-4.024232
Cacnb2	2970	-4.6388793	-3.9718573

Table 10. Top 20 overlapped and up-regulated mRNAs in mouse astrocytes stimulated with IL-9 (50 ng/ml) for 3 h and 6 h *in vitro*

Gene symbol	Gene length	up-regulated fold	
		3 h/DMEM	6 h/DMEM
Ccl2	806	3.1756024	9.821831
Nrxn1	9040	2.2285407	9.118354
Ereg	4136	2.6865191	6.7909007
Ccl7	912	2.5141113	6.3414073
Fpr1	1332	6.2122507	5.5888267
Lrrc55	2900	2.7651134	5.2560782
Bcl11b	7923	2.5492954	5.0328083
Cxcl2	1083	4.2408137	4.948825
Klrb1c	2641	3.2704635	4.811274
Tnf	1619	5.9117227	4.6778245
Chm	4867	2.8186088	4.4003916
Rnf20	4159	3.6893559	4.212892
6430704M03Rik	3854	2.0068235	4.1690726
Gbp6	5548	2.0744424	3.9634035
Ak4	4894	2.5767694	3.9619064
Tcstv3	878	6.379969	3.6716871
4930415L06Rik	2618	2.5779061	3.394951
Ajap1	3067	4.3802185	3.2806315
Vsig8	1814	2.9814172	3.2300596
Itch	5214	3.3478744	3.229839

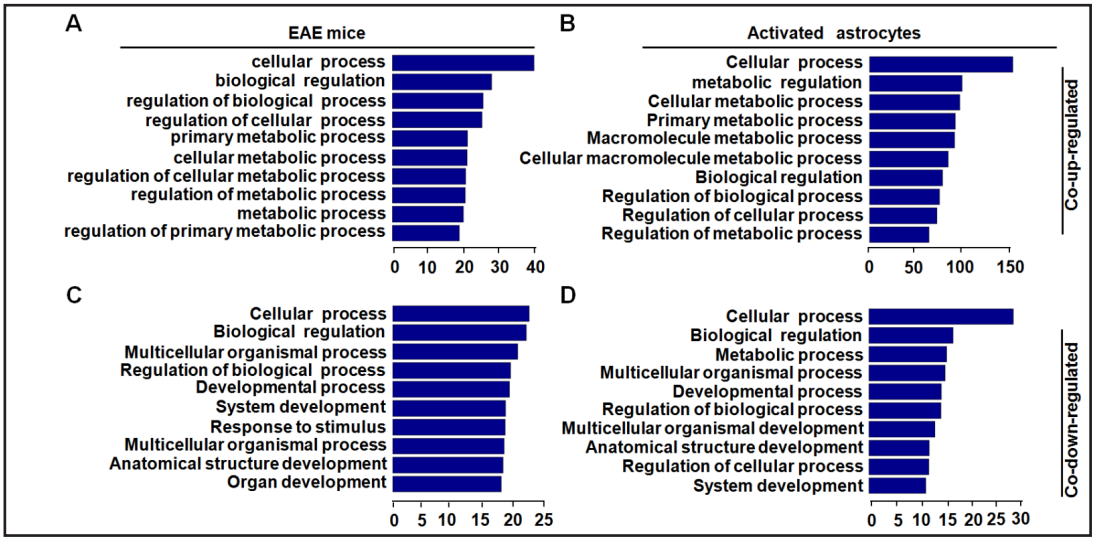

Fig. 6. Biological functions of differential overlap genes with fold changes > 2.0. (A and B) The significant biological process, cellular component and molecular function of co-up-regulated genes or co-down-regulated genes were shown in the brain tissues of EAE mice with clinical scale 1 and scale 4. (C and D) Significantly enriched molecular function, biological process and cellular component of co-up-regulated genes or co-down-regulated genes were identified in the activated astrocytes stimulated by IL-9 for 3 h and 6 h.

KEGG Pathway analysis showed that 40 pathways were significantly enriched among differentially expressed genes. Co-up-regulated genes in the brain tissues of EAE mice with clinical scale 1 and scale 4 were related to glutamatergic synapases, calcium signaling pathways, retrograde endocannabinoid signaling, adherens junctions, leukocyte transendothelial migration and so on (Fig. 7A). The co-down-regulated genes in EAE mice were involved in the renin-angiotensin system, African trypanosomiasis, malaria, neuroactive ligand-receptor interaction, etc (Fig. 7B). Similarly, KEGG Pathway results indicated that the co-up-regulated genes in the activated astrocytes stimulated by IL-9 for 3 h and 6 h were involved in PI3K-Akt signaling pathway, focal adhesion, adherens junctions, regulation of actin cytoskeleton, etc (Fig. 7C). Furthermore, the co-down-regulated genes in

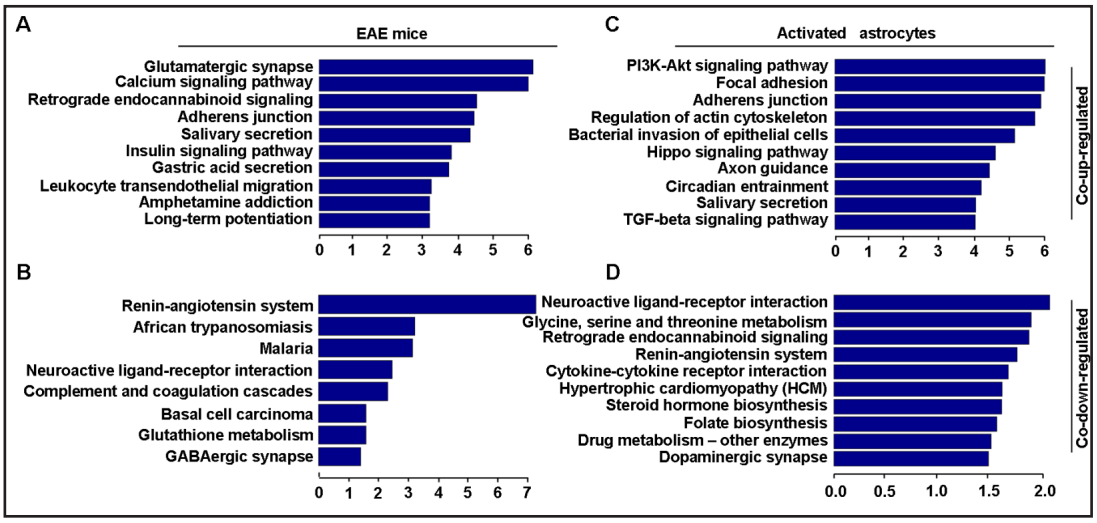

Fig. 7. KEGG Pathway analysis of differential overlap genes with fold changes >2.0. (A) The significant pathways for co-up-regulated genes in the brain tissues of EAE mice with clinical scale 1 and scale 4. (B) The remarked pathways for co-down-regulated genes in the brain tissues of EAE mice. (C) The significant pathways for co-up-regulated genes in astrocytes stimulated by IL-9 for 3 h and 6 h. (D) The significant pathways for co-down-regulated genes in astrocytes stimulated by IL-9 for 3 h and 6 h.

the activated astrocytes were involved in neuroactive ligand-receptor interaction, glycine, serine and threonine metabolism, retrograde endocannabinoid signaling, renin-angiotensin system, etc (Fig. 7D).

Table 11. Top 20 overlapped and down-regulated mRNAs in mouse astrocytes stimulated with IL-9 (50 ng/ml) for 3 h and 6 h *in vitro*

Gene symbol	Gene length	down-regulated fold	
		3 h/DMEM	6 h/DMEM
Enox1	3089	-59.50836	-59.80875
Pcdh15	8923	-18.557398	-20.820673
Ikzf1	4902	-30.949173	-17.208952
Traf3ip3	2142	-6.6899185	-16.649658
Apcs	1012	-3.031945	-8.404199
Gm4975	3739	-5.5699153	-7.644075
Ptpn6	2222	-5.612801	-7.551555
Ttc5	1841	-7.556124	-7.4247823
1700034I23Rik	2345	-7.4411135	-6.9960046
Gemin5	6226	-7.5955577	-6.9607325
Htr3a	2089	-3.7103636	-6.669303
Ankrd43	3644	-9.93209	-6.5875645
Zfp707	1816	-3.1428037	-6.012515
Pdia4	2610	-5.130527	-5.9437757
Ccdc27	2084	-3.5900488	-5.61525
Ido1	1555	-3.8029835	-5.471567
1700021F07Rik	641	-4.75571	-5.203718
Dhx57	5094	-8.452597	-5.2024207
Slamf1	2688	-7.1919804	-5.177014
Olfr91	939	-2.9942255	-5.0656576

Discussion

MS/EAE is a chronic autoimmune disease of the central nervous system with inflammation, demyelination and axon degradation. Many studies have demonstrated that the blockade of pro-inflammatory cytokines production in astrocytes can attenuate the damage of MS/EAE [19-21].

Over the past decades, the molecular mechanisms underlying MS have been extensively studied. However, our understanding of the pathophysiological process of MS is still incomplete. In recent years, lncRNAs have received much attention in human diseases. Aberrant expression or function of lncRNAs have been linked to cancer, neurological disorders, and hemolysis, elevated liver enzymes and low platelets (HELLP) syndrome [18, 22, 23]. Moreover, lncRNAs are important regulators of immune cells differentiation and function, eg. T cells, dentritic cells, B cells, macrophages and NK cells [24]. Emerging evidence indicates that lncRNAs not only participate in autoimmune diseases including systemic lupus erythematosus (SLE), rheumatoid arthritis (RA) and psoriasis [25-27], but also play important roles in CNS development, homeostasis, stress responses, and plasticity [28]. Recent work points to the role of lncRNAs in oligodendrocyte precursor cell (OPC) differentiation from neural stem cells (NSCs), myelination and remyelination in the CNS [29, 30]. lncRNA (Malat1) displays

anti–apoptotic and anti-inflammatory roles in microvasculature structure of the brain to reduce ischemic brain injury [31]. However, there is a large gap between the number of existing lncRNAs and their known association with a particular molecular or cellular function in MS/EAE. To date, the functional characterization of lncRNAs during the EAE progression and astrocyte activation has not been carried out systematically. In the present study, we explored the expression profiles of lncRNAs and mRNAs both in the brain tissues of EAE mice and in IL-9-induced astrocytes, analyzed the co-expression of lncRNAs *in vivo* and *in vitro*, and inferred their characteristics and possible relations with protein-coding genes.

There were 1, 850 up-regulated lncRNAs and 1, 642 up-regulated mRNAs in the brain tissues of EAE mice. Meanwhile 1, 450 lncRNAs and 1, 608 mRNAs were down-regulated. Furthermore, 1, 584 lncRNAs and 1, 435 mRNAs were up-regulated, and 2, 164 lncRNAs and 1, 897 mRNAs were down-regulated in the astrocytes stimulated by IL-9 for 3 h and 6 h. Notably, there were 2 lncRNAs that differentially co-up-regulated and 3 lncRNAs that differentially co-down-regulated both in the brain tissue of EAE mice and in activated astrocytes. There were 7 mRNAs co-up-regulated and 2 mRNAs co-down-regulated both in the brain tissues from EAE mice and in activated astrocytes. Moreover, real-time PCR were performed to verify part of results in EAE mice and in activated astrocytes, which was consistent with the results of lncRNAs microarray. These altered lncRNAs revealed a close association with the levels of inflammatory cytokines secreted by activated astrocytes and severity of EAE mice, suggesting these lncRNAs might provide novel insight into the molecular basis of MS/EAE.

A number of inflammation-related genes were dramatically co-up-regulated in EAE mice and in activated astrocytes, such as c*xcl10 (IP-10)*, *cxcl2, ccl2* and *tnf.* Furthermore, some mRNAs including complement factor B, Transthyretin, LIM homeobox protein 6, G-protein coupled receptor 84 (Gpr84) and Fatty acid binding protein 4 were also screened out and remarkably increased both *in vivo* and *in vitro* (Table 8 and 10), whose functions are unclear in the brain tissue of EAE mice. Further studies are needed to identify whether they are involved in EAE processing.

It has been established that lncRNAs are involved in the regulation of the immune system, including NF-κB signaling, anti-viral response, $CD4^+$ and $CD8^+$ T-cell differentiation and inflammatory response [18]. Based on the GO term enrichment and pathway maps of mRNAs, we found that markedly enriched molecular functions and biological processes of up-regulated gene in EAE mice were mainly involved in metabolism regulation, biological regulation, biological process regulation and inflammation. These findings are consistent with previous studies showing that the infiltration of immune cells and inflammations play an important role in the induction and maintenance of MS/EAE [19].

Conclusion

In summary, our results revealed that lncRNA transcripts were highly enriched and thousands of lncRNAs were differentially expressed in the brain tissues of EAE mice and in activated astrocytes. These lncRNAs were observed to share intergenic, sense overlap, antisense overlap, or bidirectional mRNAs in genome, which may regulate their related protein-genes expression and play key roles in the pathogenesis of EAE. Further studies on these lncRNAs are required to clarify their molecular and cellular functions and determine whether they can serve as potential therapeutic targets in EAE.

Acknowledgements

This work was supported by the Natural Science Foundation of Jiangsu Province (BK20151168 to Liu, BK20141136 to Zhou), Dean Special Foundation of Xuzhou Medical University (2012KJZ10 to Liu), Xuzhou Technology Bureau Foundation (KC14SH074 to

Liu), Jiangsu Key Laboratory of Brain Disease Bioinformation to Liu (2015KF01), Jiangsu Key Laboratory Foundation of New Drug Research and Clinical Pharmacy to Liu, the Priority Academic Program Development of Jiangsu Higher Education Institutions (2014 PAPD), the National Natural Science Foundation of China (81501762 to Pan, 81461138036 to Sun), the Natural Science Foundation of the Jiangsu Higher Education Institutions (15KJB310025 to Pan) and the Graduate Innovation Program in Science and Technology of Jiangsu Province (KYLX16_1132 to Wang). Moreover, we would like to thank Jessica M. Meves (University of California San Diego) for reviewing this manuscript.

Disclosure Statement

None of the authors have any conflicts of interest in this study.

References

1 Steinman L: Immunology of relapse and remission in multiple sclerosis. Annu Rev Immunol 2014;32:257-281.
2 Hauser SL, Oksenberg JR: The neurobiology of multiple sclerosis: Genes, inflammation, and neurodegeneration. Neuron 2006;52:61-76.
3 Jager A, Dardalhon V, Sobel RA, Bettelli E, Kuchroo VK: Th1, th17, and th9 effector cells induce experimental autoimmune encephalomyelitis with different pathological phenotypes. J Immunol 2009;183:7169-7177.
4 Li H, Nourbakhsh B, Ciric B, Zhang GX, Rostami A: Neutralization of il-9 ameliorates experimental autoimmune encephalomyelitis by decreasing the effector t cell population. J Immunol 2010;185:4095-4100.
5 Zhou Y, Sonobe Y, Akahori T, Jin S, Kawanokuchi J, Noda M, Iwakura Y, Mizuno T, Suzumura A: Il-9 promotes th17 cell migration into the central nervous system via cc chemokine ligand-20 produced by astrocytes. J Immunol 2011;186:4415-4421.
6 Sofroniew MV, Vinters HV: Astrocytes: Biology and pathology. Acta Neuropathol 2009;119:7-35.
7 Wilson EH, Weninger W, Hunter CA: Trafficking of immune cells in the central nervous system. J Clin Invest 2010;120:1368-1379.
8 Haroon F, Drogemuller K, Handel U, Brunn A, Reinhold D, Nishanth G, Mueller W, Trautwein C, Ernst M, Deckert M, Schluter D: Gp130-dependent astrocytic survival is critical for the control of autoimmune central nervous system inflammation. J Immunol 2011;186:6521-6531.
9 Skripuletz T, Hackstette D, Bauer K, Gudi V, Pul R, Voss E, Berger K, Kipp M, Baumgartner W, Stangel M: Astrocytes regulate myelin clearance through recruitment of microglia during cuprizone-induced demyelination. Brain 2012;136:147-167.
10 Giraud SN, Caron CM, Pham-Dinh D, Kitabgi P, Nicot AB: Estradiol inhibits ongoing autoimmune neuroinflammation and nf b-dependent ccl2 expression in reactive astrocytes. Proc Natl Acad Sci U S A 2010;107:8416-8421.
11 Lee JT: Epigenetic regulation by long noncoding rnas. Science 2012;338:1435-1439.
12 Fatica A, Bozzoni I: Long non-coding rnas: New players in cell differentiation and development. Nat Rev Genet 2014;15:7-21.
13 Mercer TR, Dinger ME, Mattick JS: Long non-coding rnas: Insights into functions. Nat Rev Genet 2009;10:155-159.
14 Gibb EA, Vucic EA, Enfield KS, Stewart GL, Lonergan KM, Kennett JY, Becker-Santos DD, MacAulay CE, Lam S, Brown CJ, Lam WL: Human cancer long non-coding rna transcriptomes. PloS one 2011;6:e25915.
15 Qureshi IA, Mehler MF: Emerging roles of non-coding rnas in brain evolution, development, plasticity and disease. Nat Rev Neurosci 2012;13:528-541.
16 Johnson R: Long non-coding rnas in huntington's disease neurodegeneration. Neurobiol Dis 2012;46:245-254.
17 Atianand MK, Fitzgerald KA: Long non-coding rnas and control of gene expression in the immune system. Trends in Mol Med 2014;20:623-631.

18 Hrdlickova B, Kumar V, Kanduri K, Zhernakova DV, Tripathi S, Karjalainen J, Lund RJ, Li Y, Ullah U, Modderman R, Abdulahad W, Lahdesmaki H, Franke L, Lahesmaa R, Wijmenga C, Withoff S: Expression profiles of long non-coding rnas located in autoimmune disease-associated regions reveal immune cell-type specificity. Genome Med 2014;6:88.

19 Liu XM, He FX, Pang RR, Zhao D, Qiu W, Shan K, Zhang J, Lu YL, Li Y, Wang YW: Interleukin-17 (il-17)-induced microrna 873 (mir-873) contributes to the pathogenesis of experimental autoimmune encephalomyelitis by targeting a20 ubiquitin-editing enzyme. J Biol Chem 2014;289:28971-28986.

20 Kang Z, Altuntas CZ, Gulen MF, Liu C, Giltiay N, Qin H, Liu L, Qian W, Ransohoff RM, Bergmann C, Stohlman S, Tuohy VK, Li X: Astrocyte-restricted ablation of interleukin-17-induced act1-mediated signaling ameliorates autoimmune encephalomyelitis. Immunity 2010;32:414-425.

21 Yun HM, Park KR, Kim EC, Hong JT: Prdx6 controls multiple sclerosis by suppressing inflammation and blood brain barrier disruption. Oncotarget 2015;6:20875-20884.

22 Prensner JR, Iyer MK, Sahu A, Asangani IA, Cao Q, Patel L, Vergara IA, Davicioni E, Erho N, Ghadessi M, Jenkins RB, Triche TJ, Malik R, Bedenis R, McGregor N, Ma T, Chen W, Han S, Jing X, Cao X, Wang X, Chandler B, Yan W, Siddiqui J, Kunju LP, Dhanasekaran SM, Pienta KJ, Feng FY, Chinnaiyan AM: The long noncoding rna schlap1 promotes aggressive prostate cancer and antagonizes the swi/snf complex. Nat Genet 2013;45:1392-1398.

23 Wapinski O, Chang HY: Long noncoding rnas and human disease. Trends Cell Biol 2011;21:354-361.

24 Fitzgerald KA, Caffrey DR: Long noncoding rnas in innate and adaptive immunity. Curr Opin Immunol 2014;26:140-146.

25 Zhang FF, Wu LL, Qian J, Qu B, Xia SW, La T, Wu YF, Ma JY, Zeng J, Guo Q, Cui Y, Yang WL, Huang JQ, Zhu W, Yao YH, Shen N, Tang YJ: Identification of the long noncoding rna neat1 as a novel inflammatory regulator acting through mapk pathway in human lupus. J Autoimmun 2016;75:96-104.

26 Wu GC, Pan HF, Leng RX, Wang DG, Li XP, Li XM, Ye DQ: Emerging role of long noncoding rnas in autoimmune diseases. Autoimmun Rev 2015;14:798-805.

27 Sigdel KR, Cheng A, Wang Y, Duan L, Zhang Y: The emerging functions of long noncoding rna in immune cells: Autoimmune diseases. J Immunol Res 2015;2015:848790.

28 Briggs JA, Wolvetang EJ, Mattick JS, Rinn JL, Barry G: Mechanisms of long non-coding rnas in mammalian nervous system development, plasticity, disease, and evolution. Neuron 2015;88:861-877.

29 Dong X, Chen K, Cuevas-Diaz Duran R, You Y, Sloan SA, Zhang Y, Zong S, Cao Q, Barres BA, Wu JQ: Comprehensive identification of long non-coding rnas in purified cell types from the brain reveals functional lncrna in opc fate determination. PLoS Genet 2015;11:e1005669.

30 He D, Wang J, Lu Y, Deng Y, Zhao C, Xu L, Chen Y, Hu YC, Zhou W, Lu QR: Lncrna functional networks in oligodendrocytes reveal stage-specific myelination control by an lncol1/suz12 complex in the cns. Neuron 2017;93:362-378.

31 Zhang X, Tang X, Liu K, Hamblin MH, Yin KJ: Long noncoding rna malat1 regulates cerebrovascular pathologies in ischemic stroke. J Neurosci 2017;37:1797-1806.